BNL-99415-2013-TECH
C-A/AP/265;BNL-99415-2013-IR

Simulation of 3Qx Resonance Driving Term Measurement with AC Dipole Excitation

Y. Luo

January 2007

Collider Accelerator Department
Brookhaven National Laboratory

U.S. Department of Energy
USDOE Office of Science (SC)

DISCLAIMER

C-A/AP/#265
January 2007

Simulation of $3Q_x$ resonance driving term measurement with AC dipole excitation

Y. Luo, M. Bai, J. Bengtsson, W. Fischer, D. Trobjevic

Collider-Accelerator Department
Brookhaven National Laboratory
Upton, NY 11973

CAD/AP/265
January 17, 2007

Simulation of $3Q_x$ resonance driving term measurement with AC dipole excitation

Y. Luo, M. Bai, J. Bengtsson, W. Fischer, D. Trbojevic
Brookhaven National Laboratory, Upton, NY 11973, USA

To further improve the luminosity in polarized proton operation of the Relativistic Heavy Ion Collider, correction of the horizontal two-third resonance is desirable, to increase the available beam-beam tune space. The long-lasting coherent beam oscillations, produced by the AC dipole, are used to measure $3Q_x$ resonance driving term h_{30000}, through the analysis of turn-by-turn beam position data. In this note, we present the results of numerical simulations, carried out to evaluate this measurement technique.

1 Introduction

To increase the tune space available for beam-beam generated tune spread, a third order resonance correction at the current working point ($Q_x = 28.685, Q_y = 29.695$) for polarized proton operation in the Relativistic Heavy Ion Collider (RHIC) is desirable [1]. At the current working point the fractional horizontal tune Q_x is constrained by the third order resonance $Q_x = 2/3$, and the tenth order resonance $Q_x = 0.7$. With Q_x close to 0.7, both luminosity and polarization suffer. A further increase in the bunch intensity requires that particles in the center of the bunch have tunes closer to $Q_x = 2/3$.

In the 2006 polarized proton run, the $3Q_x$ resonance correction at store was tested with different schemes [2]. In Ref. [3], it is suggested to correct the $3Q_x$ resonance with 12 sextupole correctors in the interaction regions (IRs), and to correct the nonlinear chromaticities with the arc sextupole families. The key point for $3Q_x$ correction is to measure its resonance driving term h_{30000} [4, 5, 6, 7]. The beam decay in the vicinity of $3Q_x$ is used to measure the effectiveness of the correction [8].

In Ref. [4], the basic theory of the sextupole first order driving terms is outlined, and an algorithm is provided to extract first order driving terms from turn-by-turn (TBT) actions $J_x(N)$. With a modified Fast Fourier Transformation (FFT) technique, the betatron tune Q_x in the spectrum of x, and the $3Q_x$ peak in the spectrum of the action $J_x(N)$, can be precisely calculated [9, 10, 11]. According to Ref. [4], the peak at $3Q_x$ in the spectrum of $J_x(N)$ is linked to the $3Q_x$ resonance.

To be able to extract h_{30000} from TBT beam position monitor (BPM) data, a long-lasting, coherent, and large amplitude betatron oscillation is required. At 100 GeV, after 5 consecutive kicks with the tune meter kicker, the maximum oscillation amplitude of the beam center is about 1.5 mm at BPM rbpm.bo6-bh4. A disadvantage of the kicked BPM data is its fast decoherence and small amplitude. In addition, too many kicks increase the emittance significantly.

The AC dipole has been proven to be a powerful tool to produce long-lasting coherent beam oscillations with large amplitude. If the driving strength of AC dipole is ramped up and down adiabatically, no significant emittance increase is observed [12]. The TBT BPM data taken at the flattop of AC dipole excitation can be used for linear as well as nonlinear lattice measurements [13, 6, 7].

In the following, we first review the sextupole driving term theory and the data processing procedure to extract h_{30000} from TBT BPM data. Then, we simulate the AC dipole excitation to measure the h_{30000} under various conditions.

2 Background

2.1 First order resonance driving terms

Sextupoles give rise to the following first order geometric driving terms,

$$h_{21000} = -\frac{1}{8}\sum_{i=1}^{N}(k_2 dl)_i \beta_{x,i}^{3/2} e^{i\mu_{x,i}}, \tag{1}$$

$$h_{30000} = -\frac{1}{24}\sum_{i=1}^{N}(k_2 dl)_i \beta_{x,i}^{3/2} e^{i3\mu_{x,i}}, \tag{2}$$

$$h_{10110} = \frac{1}{4}\sum_{i=1}^{N}(k_2 dl)_i \beta_{x,i}^{1/2} \beta_{y,i} e^{i\mu_{x,i}}, \tag{3}$$

$$h_{10020} = \frac{1}{8}\sum_{i=1}^{N}(k_2 dl)_i \beta_{x,i}^{1/2} \beta_{y,i} e^{i(\mu_{x,i}-2\mu_{y,i})}, \tag{4}$$

$$h_{10200} = \frac{1}{8}\sum_{i=1}^{N}(k_2 dl)_i \beta_{x,i}^{1/2} \beta_{y,i} e^{i(\mu_{x,i}+2\mu_{y,i})}. \tag{5}$$

They will drive the resonances Q_x, $3Q_x$, Q_x, $Q_x - 2Q_y$, and $Q_x + 2Q_y$, respectively, and are therefore called resonance driving terms. From Eqs. (1)-(5), each resonance driving term is a complex number,

$$h_{ijkl0} = A_{ijkl0} e^{i\phi_{ijkl0}}. \tag{6}$$

A_{ijkl0} and ϕ_{ijkl0} are the amplitude and phase of the driving term h_{ijkl0}, respectively.

According to Refs. [4], the perturbed betatron motion with first order resonance driving terms are:

$$\begin{aligned} J_x(N) = J_x &+ \frac{A_{21000}(2J_x)^{3/2}}{\sin(\pi Q_x)}\cos\left(\hat{\phi}_{21000} + \phi_x + 2\pi N Q_x\right) \\ &+ \frac{A_{10110}(2J_x)^{1/2}(2J_y)}{\sin(\pi Q_x)}\cos\left(\hat{\phi}_{10110} + \phi_x + 2\pi N Q_x)\right) \\ &+ \frac{3A_{30000}(2J_x)^{3/2}}{\sin(3\pi Q_x)}\cos\left[\hat{\phi}_{30000} + 3\phi_x + 2\pi N \cdot 3Q_x\right] \\ &+ \frac{A_{10020}(2J_x)^{1/2}(2J_y)}{\sin[\pi(Q_x-2Q_y)]}\cos\left[\hat{\phi}_{10020} + \phi_x - 2\phi_y + 2\pi N(Q_x - 2Q_y)\right] \\ &+ \frac{A_{10200}(2J_x)^{1/2}(2J_y)}{\sin[\pi(Q_x+2Q_y)]}\cos\left[\hat{\phi}_{10200} + \phi_x + 2\phi_y + 2\pi N(Q_x + 2Q_y)\right] \\ &+ O(k_2^2). \end{aligned} \tag{7}$$

$$\begin{aligned} J_y(N) = J_y &- \frac{A_{10020}(2J_x)^{1/2}(2J_y)}{\sin[\pi(Q_x-2Q_y)]}\cos\left[\hat{\phi}_{10020} + \phi_x - 2\phi_y + 2\pi N(Q_x - 2Q_y)\right] \\ &+ \frac{A_{10200}(2J_x)^{1/2}(2J_y)}{\sin[\pi(Q_x+2Q_y)]}\cos\left[\hat{\phi}_{10200} + \phi_x + 2\phi_y + 2\pi N(Q_x + 2Q_y)\right] \\ &+ O(k_2^2), \end{aligned} \tag{8}$$

where $J_x(N)$ and $J_y(N)$ are the horizontal and vertical actions of the Nth turn. The ϕ_x and ϕ_y are phases of the horizontal and vertical betatron oscillations. In Eqs. (7) and (8), J_x and J_y are the average actions.

2.2 Data Processing

According to Eq. (7), we can determine the amplitude and phase of the $3Q_x$ resonance driving term h_{30000} with an FFT of the TBT action $J_x(N)$. The amplitude and phase of the $3Q_x$ peak in the $J_x(N)$ spectrum are A_{3Q_x} and Φ_{3Q_x}, respectively, then:

$$A_{30000} = \kappa * \sin(3\pi Q_x)/3, \tag{9}$$

$$\phi_{30000} = \Phi_{3Q_x} - 3\phi_x, \tag{10}$$

where κ is the amplitude ratio of the Q_x and $3Q_x$ peaks in the spectrum of $J_x(N)$. Note that the Q_x peak in the spectrum of $J_x(N)$ is located at zero frequency, or at the average of $J_x(N)$. For Eq. (10), we have assumed that $3Q_x \approx p$, with p being an integer.

On either side of the RHIC IRs, there are two dual-plane BPMs, located between quadrupoles Q3 and Q4. These two BPMs are separated by a 36.2984 m long drift. A construction of the (x, p_x) and $J_x(N)$ from the 1024 turn-by-turn data at the horizontal 'x-position readings' of the BPM rbpm.bo6-bh3 was done in both h_{30000} measurements and in the following simulations. The horizontal Twiss parameters can be derived with an ellipse fitting, or a harmonic analysis with 1024 TBT (x, p_x) data.

Without betatron coupling, the coordinates (x, p_x) and the normalized coordinates (x_n, p_{xn}) are linked by a matrix $\mathbf{A}$:

$$\begin{pmatrix} x \\ p_x \end{pmatrix} = \mathbf{A} \begin{pmatrix} x_n \\ p_{xn} \end{pmatrix} = \mathbf{A} \begin{pmatrix} \sqrt{2J_x}\cos\Phi_x \\ -\sqrt{2J_x}\sin\Phi_x \end{pmatrix}, \tag{11}$$

where

$$\mathbf{A} = \begin{pmatrix} \sqrt{\beta_x} & 0 \\ -\alpha_x/\sqrt{\beta_x} & 1/\sqrt{\beta_x} \end{pmatrix} \quad \text{and} \quad \mathbf{A}^{-1} = \begin{pmatrix} 1/\sqrt{\beta_x} & 0 \\ \alpha_x/\sqrt{\beta_x} & \sqrt{\beta_x} \end{pmatrix}. \tag{12}$$

In Eq. (12), $\Phi_x = 2\pi(N-1)+\phi_x$. After transforming the coordinates (x, p_x) into the normalized coordinates (x_n, p_{xn}), the TBT action $J_x(N)$ can be constructed. The frequencies of Q_x in spectrum of x and $3Q_x$ in spectrum of $J_x(N)$ are precisely calculated with a modified FFT.

2.3 AC dipole excitation

The AC dipole has become a powerful diagnostic tool in the linear optics measurement. By exciting the beam with an AC dipole at a frequency in the vicinity of the betatron frequency, a coherent beam oscillation with large amplitude can be generated at the drive frequency. If the amplitude of the AC dipole strength is ramped up and down adiabatically, there is no significant emittance increase.

In RHIC, the AC dipole drive tune is typically $Q_d = Qx \pm 0.01$. The AC dipole strength ramps from zero to its maximum value in about 6000 turns, or 76 ms. The TBT BPM data are taken at the flattop of the AC dipole excitation. The AC dipole kick strength $\Delta\theta(N)$ at the Nth turn is given by

$$\Delta\theta(N) = \begin{cases} A_d * \cos(2\pi N Q_d + \phi_d) * N/N_{ramp}, & N \le N_{ramp} \\ A_d * \cos(2\pi N Q_d + \phi_d), & N > N_{ramp} \end{cases} \tag{13}$$

N_{ramp} is the number of turns for the AC dipole strength to ramp from zero to its maximum strength A_d. Q_d and ϕ_d are the AC dipole drive tune and initial phase.

3 Simulation Results

The driving term h_{30000} simulation of the measurements with the AC dipole excitation is obtained by the simulation code Tracy-II [14]. The used optics model is the same as the one prepared for the next polarized proton run [15]. In the model, the multipole errors in the interaction regions are not included. The first order chromaticities are calculated with a two family correction scheme only. Tab. 1 lists the beam and optics parameters used in the simulation.

Table 1: The beam and optics parameters used in the simulations.

quantity	unit	value
energy	GeV	100
normalized emittances ϵ_n, 95%	mm.mrad	15
tunes $(Q_{x,0}, Q_{y,0})$	...	(28.685,29.695)
chromaticities $(\xi_x^{(0)}, \xi_y^{(0)})$	...	(1.0,1.0)
lattice functions $\beta^*_{x,y}$ at IP6 and IP8	m	0.9
lattice functions $\beta^*_{x,y}$ at IP10, IP12, IP2, IP4	m	5.0
rms beam size σ_x at IP6 and IP8	mm	0.15
lattice fuction β_x at rbpm.bo6-bh3	m	503.94
lattice function α_x at rbpm.bo6-bh3	...	16.65
rms beam size σ_x at rbpm.bo6-bh3	mm	3.45
lattice function β_x at AC dipole	m	10.95
lattice function α_x at AC dipole	...	1.10

3.1 An example

In this example, we choose $Q_d = Q_x + 0.01 = 0.695$, $N_{ramp} = 6000$ turns, and $A_d = 5$ μrad. At the flattop of the AC dipole excitation, we obtain a maximum oscillation amplitude of about 3 mm at rbpm.bo6-bh3, equal to approximately one rms beam size σ_x there. Tab. 2 summarizes the AC dipole excitation parameters for this case.

Table 2: AC dipole excitation parameters in the simulation

quantity	unit	value
drive tune Q_d	...	0.695
ramp-up time N_{ramp}	turns	6000
maximum strength A_d	μrad	5
initial phase ϕ_d	degrees	0

Fig. 1 shows the TBT x data at rbpm.bo6-bh3. In the data processing, we only take 1024 turns of (x, p_x) data at the flattop of AC dipole excitation. Fig. 2 shows the TBT (x, p_x) data at rbpm.bo6-bh3. After fitting the TBT (x, p_x) points to an ellipse, we obtain the Twiss parameters at rbpm.bo6-bh3: $\beta_x(meas.) =$ 476.077 m, $\alpha_x(meas.) = 15.5784$. Then, according to Eq. (11), we transfer the coordinates (x, p_x) into normalized coordinates (x_n, p_{xn}). Fig. 3 shows the TBT normalized coordinates (x_n, p_{xn}).

The spectrum of x_n obtained with a FFT is shown in Fig. (4). The two largest peaks, at tunes 0.305 and 0.39, correspond to Q_d and $2Q_d$, respectively. From the modified FFT, we get $Q_d(meas.)= 0.694999$, which is exactly the given AC dipole drive tune. A peak at the betatron tune $1 - 0.685 = 0.315$ in Fig. (4) is not observed since the obtained spectrum comes from a driven oscillation at tune Q_d, after ramp-up to the full strength.

Fig. (5) shows $2J_x(N)$ turn-by-turn. The small modulations of J_x are a consequence of the lattice nonlinearities. The spectrum of $2Jx(N)$ obtained with a FFT is shown in Fig. 6. The peak of $3Q_d$ is located at tune $3 \times 0.695 - 3 = 0.085$, which corresponds to h_{30000}. Its amplitude is 2 order of magnitude smaller than the amplitude of the average J_x. Other peaks in Fig. 6 are related to other resonance driving terms.

The measurement results from the simulation are summarized in Tab. 3. With the optics model, according to Eq. (2), The analytical calculation of the driving term and phase from the model are: A_{30000}(analy.)=6.40 and phase ϕ_{30000}(analy.)= 149.3°, respectively. Comparison with the measurement from the predication gives an relative error for A_{30000} of 22.5%, and 2.7% for ϕ_{30000}.

Table 3: Measurement results from the simulation.

quantity	unit	value
time of data analysis	turns	1024
measured β_x	m	476.077
measured α_x	...	15.5784
measured drive tune Q_d from x_n	...	0.694999
measured tune $3Q_d$ from $2Jx(N)$	...	0.0849981
average $2J_x$	m.rad	1.73×10^{-8}
amplitude A_{3Q_d} from $2J_x(N)$	m.rad	2.02732×10^{-10}
amplitude A_{30000}	...	7.84
phase ϕ_{30000}	degrees	145.32

3.2 Measurement with different AC dipole excitation strengths

In the following, we present simulations to evaluate impacts of a number of the AC dipole excitation parameters. In beam experiments, a ramp-up period of 6000 turns was shown to be slow enough to avoid measurable emittance growth. This value was kept constant in the following simulations.

The maximum oscillation amplitude of the beam center is determined by the drive tune Q_d and kicking strength A_d. In the beam experiment, A_d has to be chosen properly. If A_d is too small, the h_{30000} measurement will have a large error. If A_d is too large, the beam lifetime will deteriorate. The maximum kicking

strength A_d is given by the physical and dynamic apertures. The simulation measurement results of h_{30000} with different AC dipole kick strengths are shown in Tab. 4. In the simulation, $Q_d = 0.695$.

Table 4: Measurement results with different AC dipole kick strengths.

A_d	x_{max}	Average J_x	A_{3Q_d} from $J_x(N)$ spectrum	A_{30000} measured	ϕ_{30000} measured
[μrad]	[mm]	[m.rad]	[m.rad]	[...]	[degrees]
2.5	1.38	4.33×10^{-9}	2.54×10^{-11}	7.83	150.6
5	2.87	1.73×10^{-8}	2.03×10^{-10}	7.84	145.3
10	5.76	6.89×10^{-8}	1.62×10^{-9}	7.87	142.7

3.3 Measurement with different AC dipole drive tunes

The optimum drive tune of the AC dipole was found experimentally to be $Q_d = Q_x \pm 0.01$. The maximum oscillation amplitude of the beam center is proportional to $1/|Q_d - Q_x|$. The simulation measurement results of h_{30000} with different AC dipole drive tunes are shown in Tab. 5. In the simulation, $A_d = 5$ μrad.

From Tab. 5, the measured phase of h_{30000} has not changed much when the drive tune is chosen between $Q_x - 0.015$ and $Q_x + 0.015$. However, the measured amplitude A_{30000} at $Q_d = Q_x + 0.015 = 0.700$ is rather different from that measured with $Q_d = Q_x \pm 0.01$.

Table 5: Measurement results with different AC dipole drive tunes.

Q_d	A_{30000} measured	ϕ_{30000} measured
[...]	[...]	[degrees]
0.700	14.31	148.9
0.695	7.84	145.3
0.675	8.72	151.8
0.300	14.31	149.0
0.305	7.89	145.1
0.325	8.72	151.9

3.4 Measurement with different first order chromaticities

The h_{30000} measurement results, under different first order chromaticity settings, are shown in Tab. 6. The analytical results of h_{30000} are also listed. Except for the first order chromaticities, other optics and the AC dipole excitation parameters are same as that in Tab. 1 and Tab. 2. From Tab. 6, when slightly changing the first order chromaticities, the phase of h_{30000} is almost constant while the amplitude of h_{30000} exhibits tolerable changes.

If the first order chromaticities is varied by several units, the strengths of all the chromatic sextupoles are scaled up or down simultaneously. Since the betatron phase advances between the sextupoles are unchanged, the phase of h_{30000} doesn't change and the amplitude of h_{30000} scales up or down.

Table 6: Measurements with different chromaticities.

(Q_x,Q_y)	$(\xi_x^{(0)},\xi_y^{(0)})$	A_{30000} measured	ϕ_{30000} measured	A_{30000} analytical	ϕ_{30000} analytical
[...]	[...]	[...]	[degrees]	[...]	[degrees]
(28.685,29.695)	(0.5,0.5)	7.79	145.4	6.36	149.3
(28.685,29.695)	(1.0,1.0)	7.84	145.3	6.40	149.3
(28.685,29.695)	(2.0,2.0)	7.93	145.3	6.48	149.3
(28.685,29.695)	(3.0,3.0)	8.03	145.2	6.56	149.3

3.5 Measurement in the vicinity of the $3Q_x$ resonance

The h_{30000} measurement results in the vicinity of third order resonance line $Q_x = 2/3$ are shown in Tab. 7. For each case, we only match Q_x while keeping the sextupole strengths unchanged. These sextupole strengths are calculated at tunes $(28.685, 29.695)$. Therefore the first order chromaticities presented in Tab. 7, at different Q_x are slightly different from 1. The AC dipole drive tune is always $Q_x + 0.01$.

The variations of predicated ϕ_{30000} (obtained from the analytical calculation based on Eq. (2)) for different Q_x in the vicinity of $3Q_x$ resonance line, are small, as shown in Tab. 7. And the measured ϕ_{30000} agrees well with its prections, except at $Q_x = 28.675$ and 28.6725. At these two working points, the difference in ϕ_{30000} between the measurement and the prediction is larger than 20°.

The measurements of h_{30000} in the vicinity of the third order resonance line $Q_x = 2/3$, with adjustment of the first order chromaticities are shown in Tab. 8. At each Q_x, the first order chromaticities are set to $(\xi_x^{(0)}, \xi_y^{(0)}) = (1, 1)$. A comparison between the measured and analytically calculated h_{30000}s for the same values of Q_x with and without the first order chromaticity adjustment, presented in Tab. 7 and Tab. 8, shows a close agreement.

The analytical estimate for h_{300000} in Eq.(2) is obtained by the first order perturbation theory. However, when Q_x is close to the $3Q_x$ resonance and the higher order terms will contribute. Therefore, in the vicinity of the $3Q_x$ resonance there is a relatively large discrepancy in ϕ_{30000} between the measurement and the prediction as shown in Tab. 7 and Tab. 8.

Table 7: Measurements in the vicinity of $3Q_x$ without adjustment of first order chromaticities.

(Q_x,Q_y)	$(\xi_x^{(0)},\xi_y^{(0)})$	A_{30000} measured	ϕ_{30000} measured	A_{30000} analytical	ϕ_{30000} analytical
[...]	[...]	[...]	[degrees]	[...]	[degrees]
(28.690,29.695)	(0.66,0.87)	11.69	147.7	6.46	153.7
(28.685,29.695)	(1.00,1.00)	7.84	145.3	6.40	149.3
(28.680,29.695)	(1.35,1.12)	12.57	133.0	6.34	146.2
(28.675,29.695)	(1.72,1.24)	6.74	113.6	6.29	143.1
(28.6725,29.695)	(1.90,1.30)	10.20	165.5	6.26	142.5
(28.670,29.695)	(2.08,1.36)	9.73	131.5	6.24	140.1

Table 8: Measurements in the vicinity of $3Q_x$ with adjustment of first order chromaticities.

(Q_x,Q_y)	$(\xi_x^{(0)},\xi_y^{(0)})$	A_{30000} measured	ϕ_{30000} measured	A_{30000} analytical	ϕ_{30000} analytical
[...]	[...]	[...]	[degrees]	[...]	[degrees]
(28.690,29.695)	(1.00,1.00)	11.72	147.6	6.48	152.2
(28.685,29.695)	(1.00,1.00)	7.84	145.3	6.40	149.3
(28.680,29.695)	(1.00,1.00)	12.54	133.0	6.32	146.1
(28.675,29.695)	(1.00,1.00)	6.69	113.3	6.24	143.1
(28.6725,29.695)	(1.00,1.00)	10.12	165.7	6.21	141.5
(28.670,29.695)	(1.00,1.00)	9.63	131.4	6.17	140.1

3.6 Measurement after h_{30000} correction with 12 IR sextupoles

The h_{30000} correction with the 12 sextupoles in the interaction regions is applied. The correction scheme is given in Ref. [3]. Tab. 9 lists all the first order resonance driving terms before and after the h_{30000} correction. The correction strengths for these 12 sextupoles are also listed. After correction of the h_{30000} term, the simulation measurement shows that the amplitude and phase of h_{30000} are 0.702 and 202.0°, respectively. The spectrum of $2J_x(N)$ before and after h_{30000} correction is shown in Fig. 7. The peak of $3Q_x$ after correction is about one order of magnitude smaller than that without correction. The amplitudes of other peaks have no significant change before and after h_{30000} correction.

Table 9: Analytical first order sextupole resonance driving terms before and after correction.

Before correction: (real part, imaginary part)	
h_{21000}	(2.07, -3.59)
h_{30000}	(-5.50, 3.27)
h_{10110}	(9.22, -0.87)
h_{10020}	(1.45, 6.85)
h_{10200}	(-0.59, 9.61)
After correction: (real part, imaginary part)	
h_{21000}	(2.07, -3.59)
h_{30000}	(0.00, 0.00)
h_{10110}	(9.22, -0.87)
h_{10020}	(1.45, 6.85)
h_{10200}	(-0.59, 9.61)
Strengths after correction:	
B2M06C3B	0.00051
B2M07C3B	-0.00065
B2M08C3B	-0.00182
B2M09C3B	0.00578
B2M10C3B	0.00389
B2M11C3B	0.00811
B2M12C3B	-0.00833
B2M01C3B	-0.00754
B2M02C3B	-0.00704
B2M03C3B	0.02376
B2M04C3B	0.01704
B2M05C3B	9.5e-05

3.7 Local and global observations

The measurement simulation and correction of the h_{30000} as presented above, was performed only at BPM rbpm.bo6-bh3. But h_{30000} may vary along the ring. The values of the A_{30000} obtained by analytical calculation along the ring before and after the correction arre shown in Fig. 8. The A_{30000} is almost constant in each interaction region (Fig. 8). In the arcs, regular fluctuations in A_{30000} are seen. These fluctuations indicate that perhaps contributions from arc sextupoles to h_{30000} do not cancel very well. After the correction, A_{30000} is smaller in most parts of the ring, especially in the region between the interaction regions IP4 and IP8.

4 Conclusion

We have simulated the measurement of third order resonance driving term h_{30000} with the AC dipole excitation. The simulations confirm that the AC dipole is a promising tool for the h_{30000} measurement. The theory of third order resonance driving terms and the BPM data processing algorithms were reviewed. Influence of AC dipole parameters variations, first order chromaticities, and horizontal set tunes Q_x on the h_{30000} measurement result has been evaluated. In addition the h_{30000} driving term was estimated both globally and locally, after correction with 12 IR sextupole correctors.

5 Acknowledgments

The authors would like to thank R. Calaga, F. Pilat, N. Malitsky, and C. Montag for discussion during this work. This work is support by the US DOE under contract No. DE-AC02-98CH10886.

References

[1] W. Fischer, *Beam-beam and BTF*, 2006 RHIC Accelerator Physics Experiments Workshop, November 2-3, 2005, BNL.

[2] Y. Luo, *Nonlinear chromaticities and* $3Q_x$ *resonance corrections*, 2006 RHIC Accelerator Physics Experiments Workshop, November 2-3, 2005, BNL.

[3] Y. Luo, J. Bentsson, W. Fischer, and D. Trbojevic, *Simulation of proposed on-line third order resonance correction schemes*, BNL C-AD AP Note-264, Dec., 2006.

[4] J. Bengtsson, *The sextupole scheme for the Swiss Light Source(SLS): an analytical approach*, SLS Note 9/97, March 7, 1997.

[5] R. Bartolini and F. Schmidt, *Normal form via tracking or beam data*, Part. Accel. **59**, 93(1998).

[6] F. Schmidt, R. Tomas, *Measurement of drving terms*, Proceedings of the 2001 Particle Accelerator Conference, Chicago, 2001.

[7] R. Tomas, et al., *Measurement of global and local resonance terms*, Phys. Rev. ST Accel. Beams, **8**, 024001(2005).

[8] R. Calaga and W. Fischer, private communications, 2006.

[9] E. Asseo, J. Bengtsson and M. Chanel, Proceedings of 4th European Signal Processing Conference, North Holland, Amsterdam, pp.1317-1320, 1988.

[10] J. Laskar, Physica D **67**, 257 (1993).

[11] R. Bartolini, A. Bazzani, M. Giovannozzi, W. Scandale and E. Todesco, *Precise measurement of the betatron tune*, Part. Acc. **55**, 247(1996).

[12] M. Bai, et al., *Experimental test of coherent betatron resonance excitation*, Phys. Rev. Lett. **56**, 6002, 1999.

[13] M. Bai, et al., *RHIC vertical AC dipole commissioning*, Proceedings of EPAC 2002, Paris, France.

[14] J. Bengtsson, private communications, 2006.

[15] S. Tepikian, private communications, 2006.

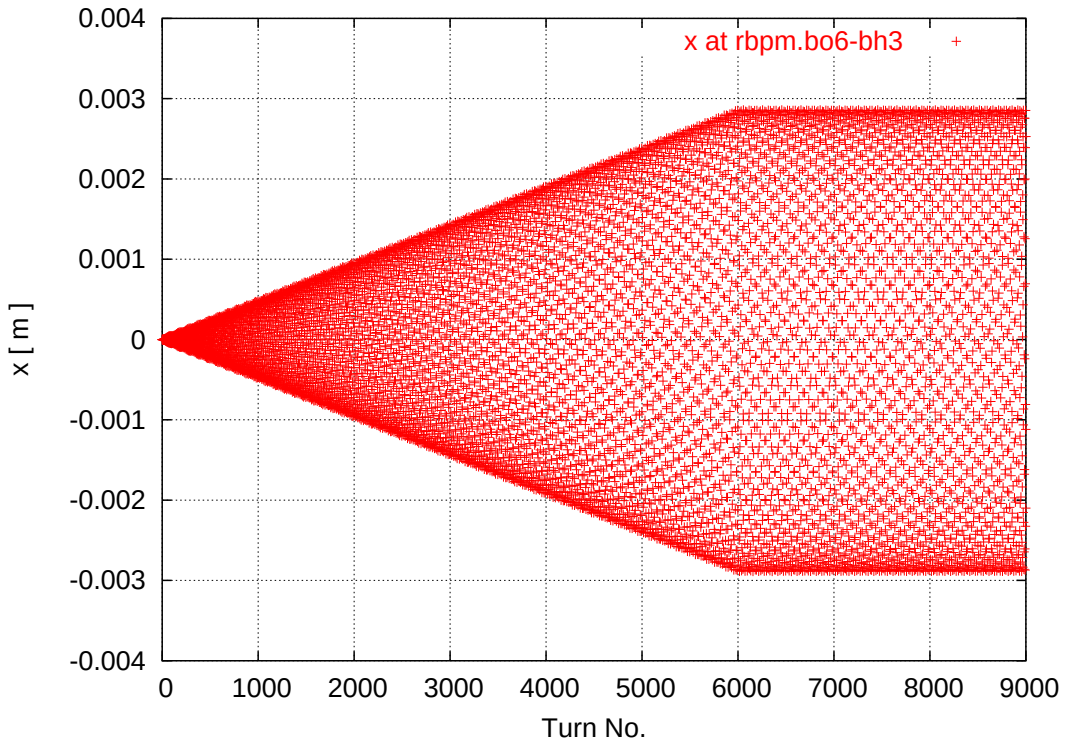

Figure 1: Turn-by-turn x data at rbpm.bo6-bh3 during ramp-up and flattop of AC dipole excitation.

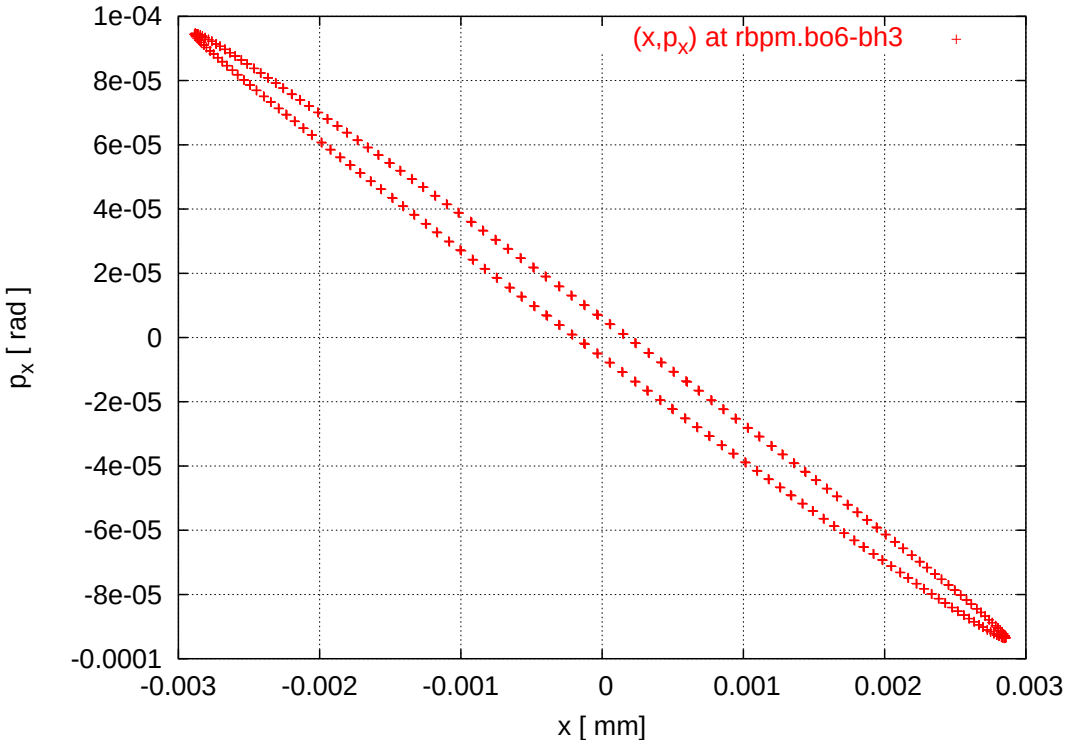

Figure 2: Turn-by-turn data (x, p_x) at rbpm.bo6-bh3 taken at the flattop of AC dipole excitation.

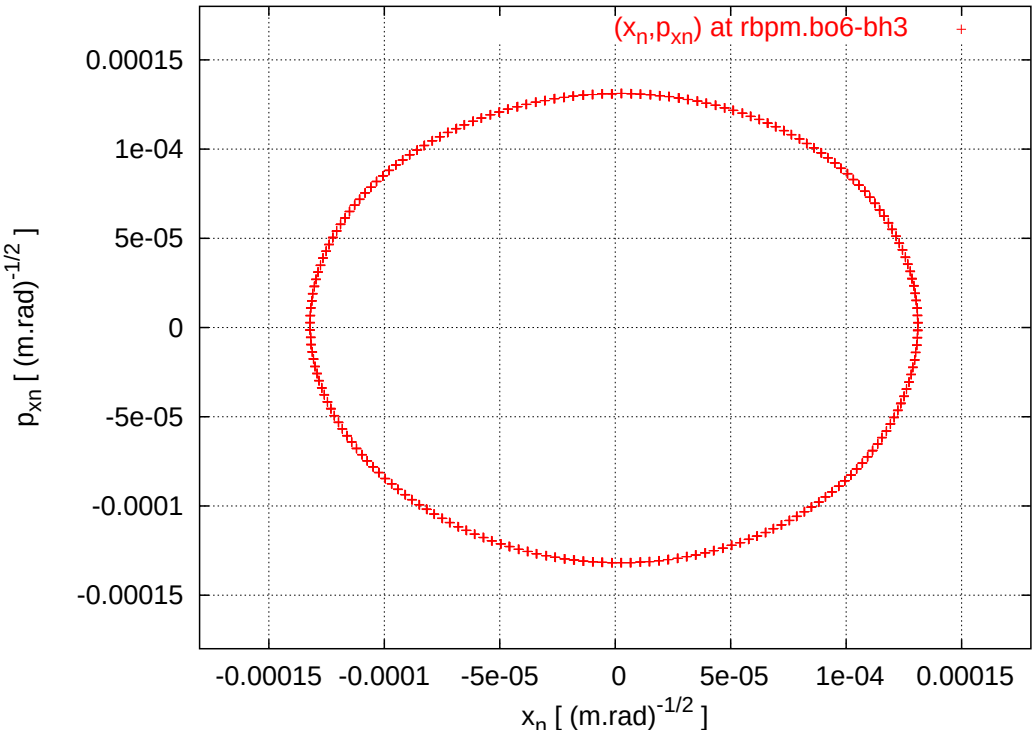

Figure 3: Turn-by-turn normalized data (x_n, p_{xn}) at rbpm.bo6-bh3 taken at the flattop of AC dipole excitation.

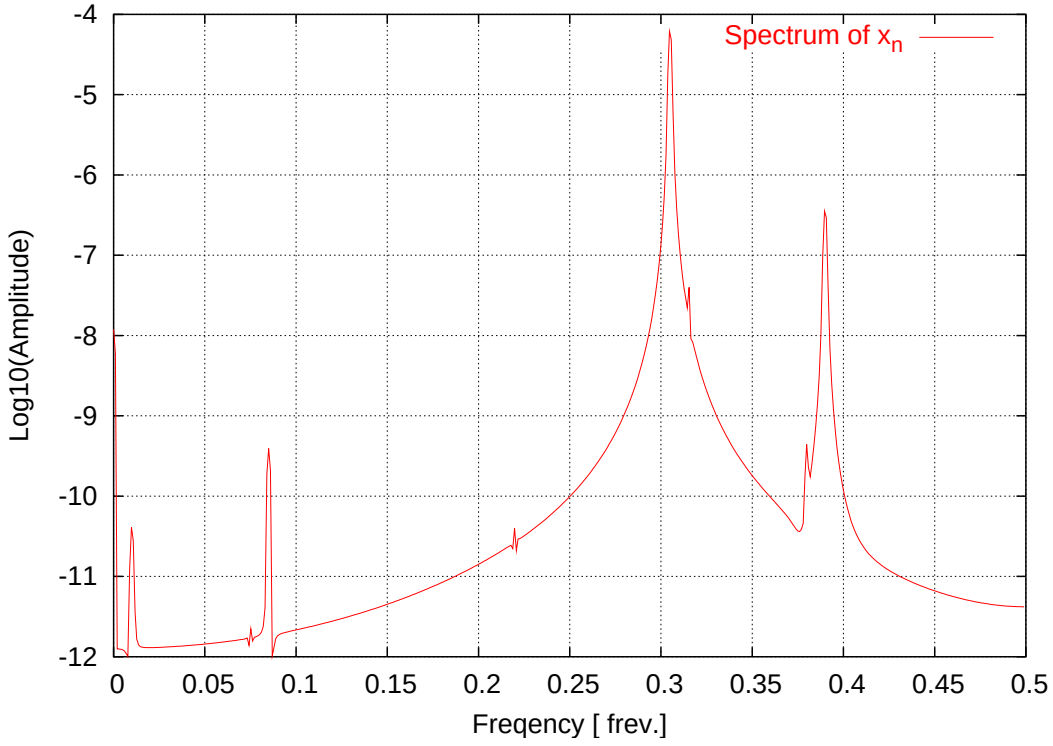

Figure 4: Spectrum of $x_n(N)$ obtained with a FFT.

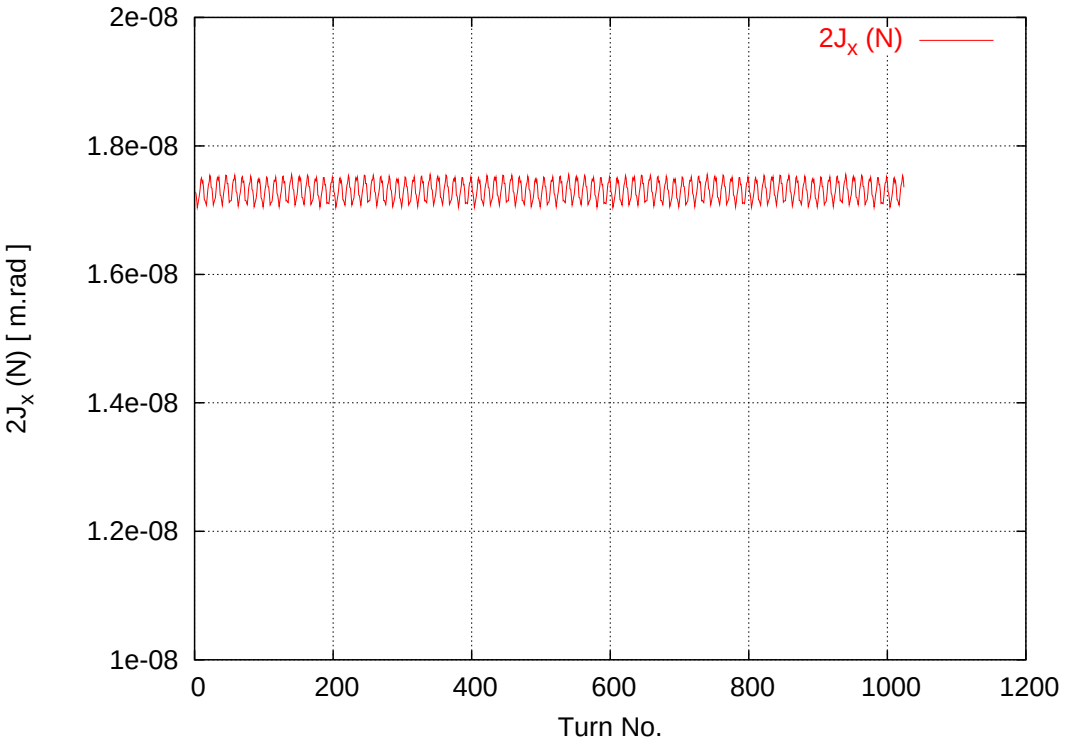

Figure 5: Turn-by-turn data $2J_x(N)$ with AC dipole excitation.

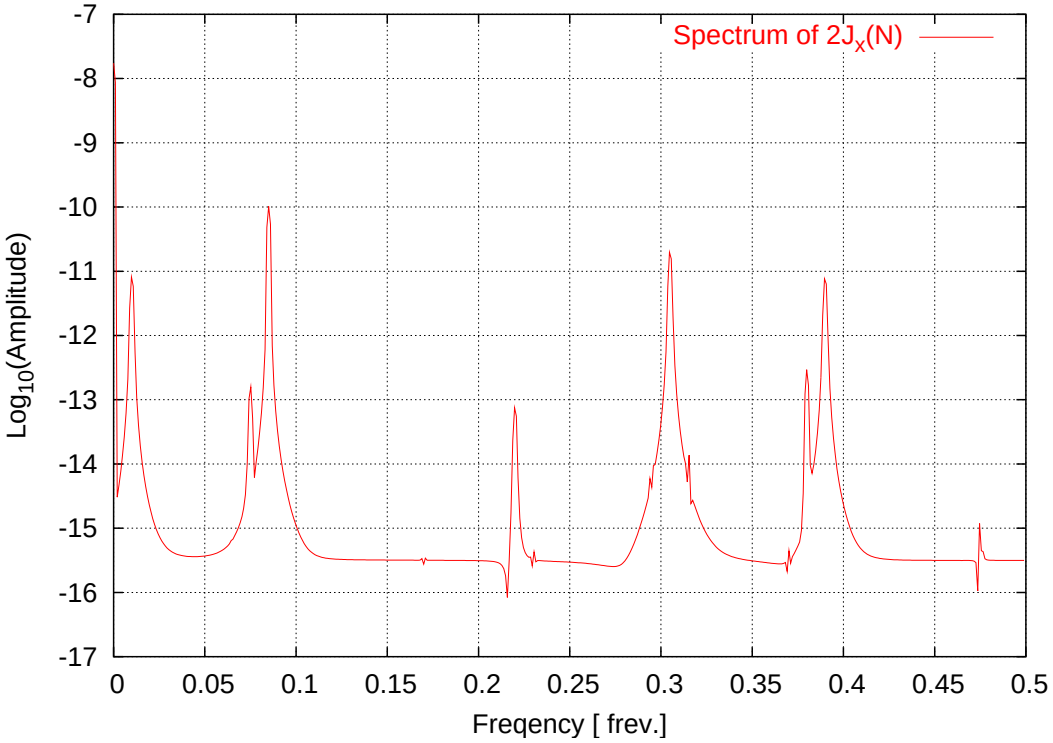

Figure 6: Spectrum of $2J_x(N)$ obtaine with a FFT.

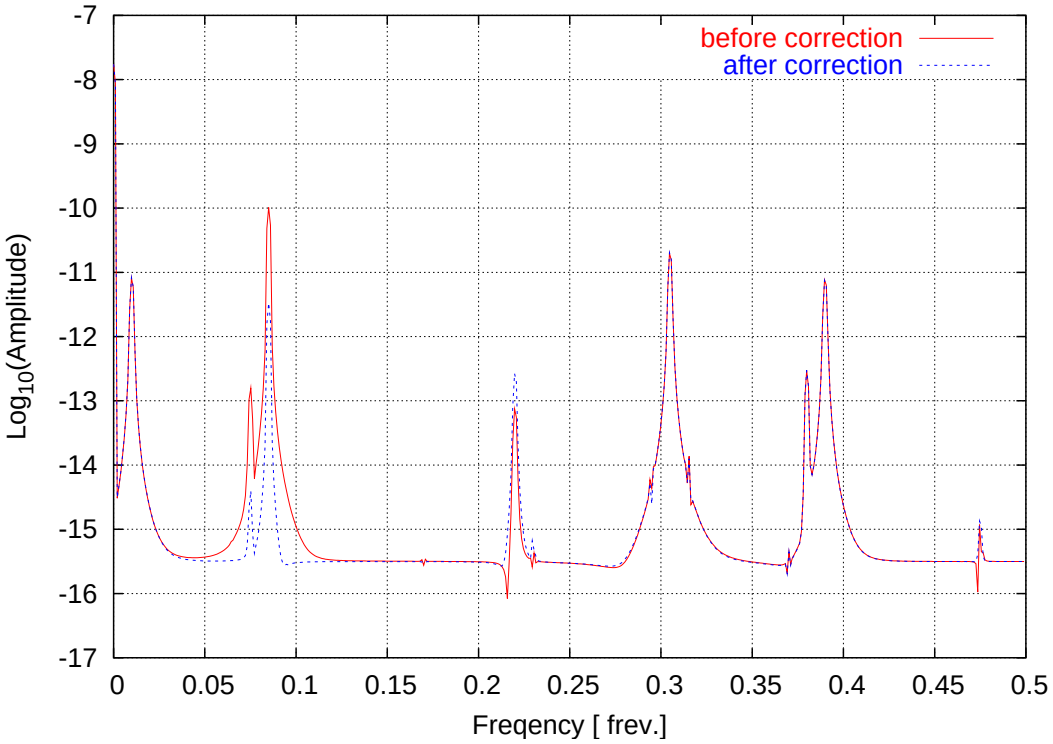

Figure 7: Spectrum of $2J_x(N)$ before and after h_{30000} correction.

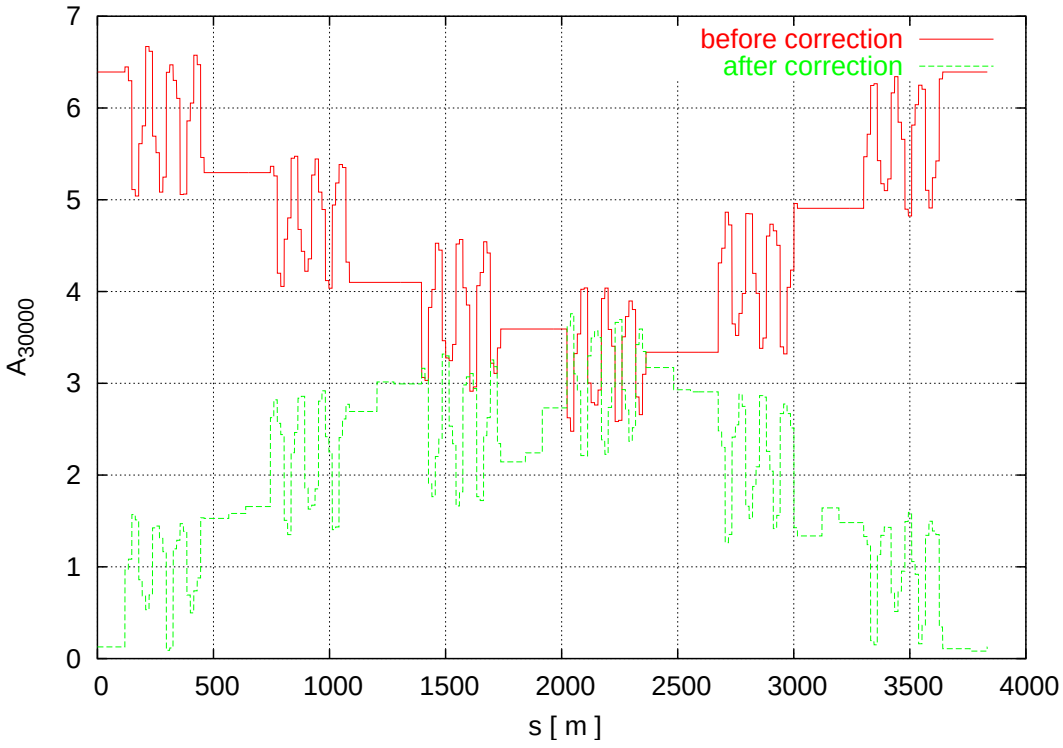

Figure 8: Analytically calculated A_{30000} along the ring before and after h_{30000} correction.